

University of Dundee

A novel, de novo mutation in PRKAG2 gene

Xu, Yanchun; Gray, Alex; Hardie, D. Grahame; Uzun, Alper; Shaw, Sunil; Padbury, James

Published in:

American Journal of Physiology - Heart and Circulatory Physiology (AJP - Heart and Circulatory Physiology)

DOI:

[10.1152/ajpheart.00813.2016](https://doi.org/10.1152/ajpheart.00813.2016)

Publication date:

2017

Document Version

Peer reviewed version

[Link to publication in Discovery Research Portal](#)

Citation for published version (APA):

Xu, Y., Gray, A., Hardie, D. G., Uzun, A., Shaw, S., Padbury, J., Phornphutkul, C., & Tseng, Y-T. (2017). A novel, *de novo* mutation in *PRKAG2* gene: infantile-onset phenotype and signaling pathway involved. *American Journal of Physiology - Heart and Circulatory Physiology (AJP - Heart and Circulatory Physiology)*, 313(2), H283-H292. <https://doi.org/10.1152/ajpheart.00813.2016>

General rights

Copyright and moral rights for the publications made accessible in Discovery Research Portal are retained by the authors and/or other copyright owners and it is a condition of accessing publications that users recognise and abide by the legal requirements associated with these rights.

- Users may download and print one copy of any publication from Discovery Research Portal for the purpose of private study or research.
- You may not further distribute the material or use it for any profit-making activity or commercial gain.
- You may freely distribute the URL identifying the publication in the public portal.

Take down policy

If you believe that this document breaches copyright please contact us providing details, and we will remove access to the work immediately and investigate your claim.

A novel, *de novo* mutation in *PRKAG2* gene: infantile-onset phenotype and signaling pathway involved

Yanchun Xu^{1,4,*}, A Gray^{2,*}, D. Grahame Hardie², Alper Uzun^{1, 4}, Sunil Shaw^{1, 4}, James Padbury^{1, 4}, Chanika Phornphutkul^{3, 4}, Yi-Tang Tseng^{1, 4, ¶}

¹Women & Infants Hospital of Rhode Island, Providence, RI, ²College of Life Sciences, University of Dundee, Dundee, Scotland, UK, ³Hasbro Children's Hospital, Providence, RI, ⁴The Warren Alpert Medical School of Brown University, Providence, RI, U.S.A.

*These authors contributed equally to this work.

Running Head: A Novel *PRKAG2* Mutation and Early-Onset Cardiac Hypertrophy.

¶Corresponding author

Contact information: Dr. Yi-Tang Tseng, 101 Dudley Street, Kilguss 122, Providence, RI 02905, U.S.A. Telephone: (401) 274-1122, x48006; Fax: (401) 277-3617; email: ytseng@wihri.org

Abstract

PRKAG2 encodes the γ 2-subunit isoform of the 5' AMP-activated protein kinase (AMPK), a heterotrimeric enzyme with major roles in regulation of energy metabolism in response to cellular stress. Mutations in *PRKAG2* have been implicated in a unique hypertrophic cardiomyopathy (HCM) characterized by cardiac glycogen overload, ventricular preexcitation and hypertrophy. We identified a novel, *de novo* *PRKAG2* mutation (K475E) in a neonate with prenatal onset of HCM. We aimed to investigate the cellular impact, signaling pathways involved and therapeutic options for K475E mutation using cells stably expressing human wild type (WT) or the K475E mutant. In HEK293 cells, the K475E mutation induced a marked increase in the basal phosphorylation of T172 and AMPK activity, reduced sensitivity to AMP in allosteric activation and a loss of response to phenformin. In H9c2 cardiomyocytes, the K475E mutation induced inhibition of AMPK and reduced response to phenformin and increases in phosphorylation of P70S6K and 4E-BP1. Primary fibroblasts from the patient with the K475E mutation also showed marked increases in phosphorylation of P70S6K and 4E-BP1, compared to those from age-matched, non-diseased controls. Moreover, overexpression of K475E induced hypertrophy in H9c2 cells which was effectively reversed by treatment with rapamycin. Taken together, we have identified a novel, *de novo* infantile-onset *PRKAG2* mutation causing HCM. Our study suggests the K475E mutation induces alteration in basal AMPK activity and results in a hypertrophy phenotype involving the mechanistic target of rapamycin (mTOR) signaling pathway, which can be reversed with rapamycin.

New & Noteworthy: We identified a novel, *de novo* *PRKAG2* mutation (K475E) in the CBS3 repeat, a region critical for AMP binding but with no previous reported mutation. Our data suggest the mutation affects AMPK activity, activates cell growth pathways and results in cardiac hypertrophy which can be reversed with rapamycin.

46

47 **Keywords:** AMPK, cardiac hypertrophy, 4E-BP1, H9c2 cells, *PRKAG2* gene mutation, p70S6K,

48 rapamycin

49

50

Introduction:

Mutations in *PRKAG2* gene, encoding the $\gamma 2$ regulatory subunit isoform of AMP-activated protein kinase (AMPK), cause a wide spectrum of cardiac phenotypes, including Wolff-Parkinson-White (WPW) syndrome (ventricular preexcitation), hypertrophic cardiomyopathy (HCM), conduction system disease, significant glycogen accumulation in myocytes and sudden death (2,6,10,18,21). AMPK is known as a cellular energy sensor and a major regulator of whole-body energy homeostasis (15). The γ subunit of AMPK is the regulatory subunit and contains four tandem repeats of a sequence called cystathionine β -synthase (CBS) motif. These motifs act in pairs to form two “Bateman domains” - binding sites for AMP and ATP (4,29). During cellular energy deficiency (increased ratio of AMP/ATP), binding of AMP to the Bateman domains activates AMPK by inducing phosphorylation of T172 in the α subunit (kinase domain) (12,13). Activation of AMPK in many tissues, including the heart, results in inhibition of ATP-consuming processes and activation of catabolic processes that favor ATP generation.

To date, many *PRKAG2* mutations have been reported. The majority of these mutations are heterozygous missense mutations within one of the four CBS domains but mutations can happen near the N-terminal, C-terminal or in a linker region between two CBS domains (Table 1).

Case presentation: We encountered a child who presented with an abnormal 27-week prenatal ultrasound, consistent with HCM. At birth, the child was noted to have significant murmur. Echocardiograms confirmed the diagnosis. Electrocardiograms revealed extremely short PR interval and combined ventricular hypertrophy (Figure 1C). Molecular testing for a hypertrophic cardiomyopathy panel revealed a novel, *de novo* likely pathogenic variant in the *PRKAG2* gene [AAA (lysine 475) to GAA (glutamic acid) or K475E]. This variant is located in the CBS3 repeat, an area that has no previous report of mutation and is conserved in all species (Table 1, Figure 1B). At three years of age, the child has modest HCM and is on supportive medication. She is otherwise developing normally. Family investigation: No family history of sudden cardiac death. Neither parent had abnormal cardiac echocardiograms or electrocardiograms. Molecular testing for *PRKAG2* in both parents was normal (Figure 1A).

To investigate the significance of the *de novo* K475E mutation on the AMPK complex, we stably expressed human *PRKAG2* wild type (WT) and K475E in HEK293 cells and H9c2

cardiomyocytes to examine AMPK activity, biochemical function and signaling pathways involved resulted from the K475E mutation. Primary fibroblasts from the patient with the K475E mutation were obtained for clinical purposes and institutional review board approval was obtained for further research study. Primary fibroblasts obtained from commercial sources and age- and sex-matched individuals were obtained and used as controls. The potential of mechanistic target of rapamycin (mTOR) inhibition as a targeted therapeutic approach for mutation-induced HCM was also investigated using the rat H9c2 embryonic cardiomyocytes. We demonstrated that the K475E mutation induced changes in the AMPK complex in a way very different from other *PRKAG2* mutations. The K475E mutation in H9c2 cells results in activation of cell growth pathways and hypertrophy, which can be attenuated by inhibition of mTOR.

Methods:

Genetic testing

Hypertrophic cardiomyopathy next generation sequencing panel testing was sent to a CLIA (Clinical Laboratory Improvement Amendments) certified laboratory (GeneDx, Gaithersburg, MD) December 2010. Genomic DNA was extracted, amplified and sequenced by solid-state sequencing - by-synthesis process. The DNA sequence was assembled and analyzed in comparison with the published genomic reference sequences. This panel included the complete coding and splice region of the following eighteen genes known to be associated with HCM: *MYH7*, *MYBPC3*, *TNNT2*, *TNNI3*, *TPM1*, *ACTC*, *MYL3*, *MYL2*, *LAMP2*, *PRKAG2*, *GLA*, *CAV3*, *MTTG*, *MTTI*, *MTTK*, *MTTQ*, *TTR*, *TNNC1*. The presence of potentially disease-associated sequence variant was confirmed by conventional dideoxy DNA sequence analysis.

Cell Culture

HEK293 and H9c2 rat fetal cardiomyocytes were grown in Dulbecco's Modified Eagle medium (Invitrogen, Carlsbad, CA) supplemented with 10% (v/v) fetal bovine serum (Atlanta Biologicals, Flowery Branch, GA) and 1% (V/V) penicillin-streptomycin (Sigma) in a humidified atmosphere containing 5% CO₂ at 37 °C. Cells were grown to 70% confluence and synchronized overnight in serum-free medium prior to experiments (33).

Institutional Research Board approval was obtained to use patients' dermal fibroblasts. Multiple age-matched control neonatal fibroblasts were obtained from commercial sources and an age- and sex-match control was obtained from the Cytogenetics Laboratory, Women & Infant's Hospital of Rhode Island. Fibroblasts were cultured in Medium 106 (Gibco) supplemented with 2% (v/v) fetal bovine serum, 2% (v/v) Low Serum Growth Supplement (LSGS) and 1% (v/v) Penicillin-streptomycin (Sigma). The final concentrations of the components in the LSGS were: hydrocortisone (1 µg/ml), human epidermal growth factor (10 ng/ml), basic fibroblast growth factor (3 ng/ml), and heparin (10 µg/ml). The cells were used between passages 2 and 6. 80-100% confluent cells were used for western blot experiment. Media was changed once daily starting at day 2 and until the termination of the experiment.

Plasmids

Full-length human WT and K475E mutant *PRKAG2* (FLAG-tagged from a tetracycline-inducible promoter) were generated as described (14) and transfected into HEK293 or H9c2 cells using Lipofectamine 2000 according to the manufacturer's instructions (Invitrogen). To establish multiple clones, individual single cells were isolated and screened for neomycin resistance.

Immunoprecipitation kinase assays of AMPK

AMPK activity was assayed using AMARA peptide on immunoprecipitated HEK293 cell lysates as described (14).

Western Blotting

Protein levels were evaluated by Western blotting as previously described (33) using phospho-specific antibodies against p70S6K1 (T-389, catalog #9234 and T-421/S-424, catalog #9204), Akt (S-473, catalog #9271 and T-308, catalog #9275), AMPK α (T172, catalog #5832) and eukaryotic translation initiation factor 4E (eIF4E)-binding protein1 (4E-BP1, T-37/46, catalog #2855; S-65, catalog #9451 and T-70, catalog #9455); and antibodies against total p70S6K1 (catalog #2708), Akt (catalog #9272), AMPK α (catalog #2531) and 4E-BP1 (catalog #9452) (Cell Signaling Technology, Danvers, MA). The intensity of bands from Western blots was scanned with densitometry and analyzed digitally with Image J software (NIH).

H9c2 cell hypertrophy and cell size measurement

H9c2 embryonic cardiomyocytes (1000 cells per 60x15 mm plate) were treated with vehicle, 200 nM Angiotensin II (AT2, Tocris, Bristol, UK), 50 nM rapamycin (Selleckchem, Houston, TX) or AT2 in combination with rapamycin for 24 hours. Cells were washed 3 times with Dulbecco's Phosphate-Buffered Saline (DPBS) then incubated with green-fluorescent Calcein AM (1 μ g/mL, Life Technologies) for 20 minutes at 37 °C. Cells were washed 5 times with DPBS. Cell size was assessed by fluorescence microscopy using an inverted microscope at 20x objective (Nikon Eclipse TE2000-E, CCD camera). Sixty to eighty random cell images were taken per plate and the cell areas were determined by Image J software. In another series of related experiments, H9c2 cells were treated with or without rapamycin for 3.5, 4, or 5 days. At each time point cells were stripped and re-plated exactly 24 hours before being harvested and stained for fluorescence microscopy. Cell

hypertrophy was also confirmed using flow cytometry. Cells were trypsinized and analyzed by flow cytometry using a FACSCanto™ system (BD Biosciences, Franklin Lakes, NJ). Forward scatter (FSC) was used to measure cell volume. For each condition 10,000 cells were counted. FSC detector gain was kept constant between samples to allow direct comparison of samples.

Statistics

Statistical significance of the differences between groups was analyzed using paired Student's *t* test or ANOVA followed by Newman-Keuls test. All data were expressed as mean \pm S.E. based on results derived from three to four independent experiments. A probability of $P < 0.05$ was considered to represent a significant difference.

Results:

Genetic testing result

The proband was found to carry a heterozygous novel missense likely pathogenic variant in *PRKAG2* gene. The nucleic acid substitution at cDNA level was c.1423 A>G resulting in amino acids alteration from lysine to glutamic acid (K475E). This change in *PRKAG2* has not been published and is not a known benign polymorphism. K475E represents a nonsynonymous substitution of negatively charged glutamic acid for positively charged lysine residue in a highly conserved across species throughout evolution and gene isoforms. In addition, in silico analysis (PolyPhen2) predicts this change to be damaging to the structure/function of the protein. Mutation affecting nearby codons (485, 487 and 488) have been published in association with cardiac hypertrophy further supporting the functional importance of this region of the protein (2,3,21). Furthermore, K475E was not observed in 704 control chromosomes of varying ethnic backgrounds tested at the laboratory, indicating it is not a common benign variant. In addition, the parents who are both clinically asymptomatic, had normal ECG and cardiac echo were not found to carry this variant. Based on this information, we concluded that the K475E in *PRKAG2* is most consistent with a *de novo* pathogenic variant.

The K475E mutation markedly increases basal AMPK activity and reduces response to phenformin in HEK293 cells

To investigate the molecular effects of the K475E mutation on the function of the AMPK complex, we generated HEK-293 cells stably expressing either the human WT or K475E mutant FLAG-tagged $\gamma 2$ from a tetracycline-inducible promoter. We have shown previously using this system that the expressed $\gamma 2$ subunit binds to the endogenous α and β subunits (primarily $\alpha 1$ and $\beta 1$ in HEK-293 cells), partially replacing the endogenous $\gamma 1$ subunit (14). Following induction with tetracycline, AMPK complexes containing the WT or K475E $\gamma 2$ subunits were immunoprecipitated from unstressed cells using anti-FLAG antibodies and their activities determined at varying AMP concentrations. When assayed in the absence of AMP, the activity of the K475E complex was 8-fold higher than that of the WT complex (Figure 2A). However, while the WT complex was allosterically activated almost 4-fold by low concentrations of AMP (half-maximal effect, 6 μ M), the K475E mutant was only modestly activated (about 50%) and then only at much higher

concentrations ($EC_{50} \approx 90 \mu M$). The different degrees of allosteric activation of the WT and K475E mutant by AMP were particularly evident when the activities were expressed relative to the activities measured in the absence of AMP (Figure 2B).

We next compared the effects of metabolic stress induced by the drug phenformin on AMPK in HEK-293 cells stably expressing WT $\gamma 2$, the K475E mutation, or another $\gamma 2$ mutation (R531G), which is associated with an inherited form of hypertrophic cardiomyopathy with childhood onset (11). The WT, K475E or R531G complexes were immunoprecipitated using anti-FLAG antibodies and their activities measured at optimal AMP concentration (200 μM). As expected, phenformin caused a 4-fold increase in WT AMPK activity that was associated with a similar increase in T172 phosphorylation (Figure 3). As reported previously (14), complexes containing the R531G mutation exhibited modest (1.5-2-fold) increases in basal activity and T172 phosphorylation compared with the WT (although these differences were not statistically significant in this dataset), but there were no further increases in these parameters in response to phenformin. By contrast, complexes containing the K475E mutation exhibited large increases in basal activity and T172 phosphorylation (5- and 7-fold, respectively) compared to the WT, although once again there were no further increases in these parameters in response to phenformin (Figure 3). Thus, the K475E mutation yields a much larger increase in basal and kinase activity and T172 phosphorylation than the R531G mutation, but like the latter has a greatly reduced sensitivity to AMP and/or ADP, both for allosteric activation and for enhanced T172 phosphorylation.

We also used atomic co-ordinates from crystal structures of partial AMPK complexes with bound AMP, ADP or ATP (9,31), to examine the location of K475 with respect to these regulatory nucleotides. The available structures are of complexes containing $\gamma 1$ rather than $\gamma 2$, but K475 is conserved in rat $\gamma 1$ as K242. Interestingly, the nitrogen atom on the K242 side chain is within 4-5 Å of free oxygen atoms of the α -, β - or γ -phosphate groups of AMP, ADP or ATP bound in site 1 (Figures 4A-C), suggesting that K242 forms electrostatic interaction with phosphate groups of all three nucleotides. We also noted that K242 was located close to R223, a residue within the CBS3 repeat that is conserved in all vertebrate γ subunit sequences. Although the side chain of R223 points away from K242 (and the nucleotide phosphate groups) in the structures determined, if K475 was replaced with glutamate it seems feasible that the side chain of R223 could rotate to form a salt bridge with it.

Database searches showed that a lysine equivalent to K242 or K475 is conserved in all vertebrate $\gamma 1$ and $\gamma 2$ isoforms (illustrated by the human and chicken sequences), and in *Drosophila melanogaster*, *Caenorhabditis elegans* ($\gamma 1$ isoform) and *Giardia lamblia* (Figures 4D, Figure 1B). In vertebrate $\gamma 3$ isoforms and in some other invertebrate orthologues there is another basic residue (arginine) at this position. Figure 4D also shows that a basic residue is not conserved at this position in fungi (*Schizosaccharomyces pombe* and *Saccharomyces cerevisiae*) or higher plants (*Arabidopsis thaliana*); interestingly, the orthologues in these species are not allosterically activated by AMP.

The K475E mutation decreases AMPK activity, reduces response to phenformin and induces hypertrophy in H9c2 cells

Since we are studying a human gene mutation causing HCM, it would be informative to examine changes in AMPK induced by the K475E mutation in a cardiac context. Multiple individual clones of H9c2 cells stably expressing either the WT or K475E mutant were established and Western blots were performed on cell lysates. The WT and K475E expressing H9c2 cardiomyocytes were treated with or without phenformin for 1, 4, or 24 hours. In vehicle controls, the K475E- expressing cells had significantly reduced phosphorylation of AMPK α (T172), compared to WT- expressing cells (Figure 5A & B). Phenformin induced significantly increases in AMPK α phosphorylation in all the time points tested in both the WT- and K475E- expressing cells. The effect of phenformin, however, was significantly reduced in the K475E- expressing cells, compared to the WT- expressing cells (Figure 5A & B). The cell size difference between the WT- and K475E-expressing H9c2 cells was analyzed using flow cytometry. We found a small but noticeable increase in cell size of the K475E mutant-expressing cells as compared to WT-expressing cells (Figure 5C).

Effects of K475E mutation on p70S6K, Akt and 4E-BP1 in H9c2 cardiomyocytes and primary fibroblasts

Western blots were performed on cell lysates from H9c2 cell expressing the WT or K475E. As shown in Figure 6, K475E-expressing cells had significantly increased phosphorylation of p70S6K and 4EBP1, compared to the WT-expressing cells. Phosphorylation at T-389 is critical for p70S6K activation and is considered rapamycin-sensitive (7). 4E-BP1, a translation repressor protein,

inhibits cap-dependent translation by binding to eIF4E. Phosphorylation of 4E-BP1 at multiple residues leads to its dissociation from eIF4E thus results in activation of cap-dependent mRNA translation (25). Therefore, phosphorylation of p70S6K and 4E-BP1 was used as readout for cellular growth. Phosphorylation of 4E-BP1 at T37/T46, S65 and T70 were all significantly increased in K475E-expressing cells, compared to WT-expressing cells (Figure 6). In contrast, Akt phosphorylation (S473, T308) was not changed.

Western blot experiments described above were repeated using primary fibroblast from the patient with the K475E mutation and multiple age- and sex-matched controls. Similarly, fibroblasts carrying the K475E mutation had significant increases in phosphorylation of p70S6K and 4E-BP1, compared to the controls (Figure 7). Again, phosphorylation of Akt was not changed.

Taken together, these results suggest the K475E mutation results in an Akt-independent activation of cell growth pathway.

Inhibition of mTOR by rapamycin reversed angiotensin II-induced H9c2 cell hypertrophy and the K475E cardiac phenotype *in vitro*

Induction of H9c2 cell hypertrophic responses by angiotensin II (Ang II) has been demonstrated to be similar to those in primary neonatal cardiomyocytes (30). To examine if inhibition of mTOR can reverse Ang II-induced hypertrophy, WT- and K475E-expressing cells were treated with vehicle, Ang II alone, rapamycin alone or Ang II + rapamycin for 24 hours. Cells were immunofluorescence-stained and cell areas were assessed by microscopy. In all treatment groups including the vehicle control group, the K475E-expressing H9c2 cells had a significant increase in cell size, compared to the WT-expressing cells (Figure 8). Ang II treatment induced hypertrophy in both WT- and K475E-expressing cells. Rapamycin treatment alone did not change cell size but effectively abrogated cell hypertrophy induced by Ang II. These results demonstrate mTOR inhibition by rapamycin can reverse Ang II-induced cell hypertrophy in both WT- and K475E-expressing H9c2 cells, but fails to ‘rescue’ the K475E phenotype as the K475E-expressing cell size remained significantly increased, compared to the WT-expressing cells, in all treatment groups.

One possibility for the lack of phenotype ‘rescue’ following rapamycin treatment is that a 24-hour treatment regimen may not be sufficient. We therefore examined the time-course effect of rapamycin on H9c2 cell hypertrophy. The WT- and K475E-expressing cells were treated with or

without rapamycin for 1, 3.5, 4, or 5 days. In both cell groups, cell size increased significantly after longer incubation time (over 3.5 Days, Figure 9A). While the cell size of WT-expressing cells reached a plateau at day 3.5, those of K475E-expressing continued to increase. In WT-expressing cells, treatment of rapamycin effectively reduced the increases in cell size on days 3.5 and 4 but the effect seemed to taper off on day 5. In contrast, the effect of rapamycin remained effective in reducing the size of K475E-expressing cells with the effect becoming even more obvious at day 5 when the cell sizes of rapamycin-treated K475E-expressing cell were comparable to that of WT-expressing cells at day 5 (Figure 9B). Taken together, these data demonstrated mTOR inhibition by rapamycin can be an effective therapeutic approach for K475E mutation induced hypertrophy.

Discussion:

Mutations in *PRKAG2* induce a wide range of cardiac phenotypes, including glycogen overload, ventricular preexcitation, conduction diseases and hypertrophy. Many mutations have an early-onset cardiac phenotype, as the case for K475E. Given that identification of this disease can be challenging (patient with an infantile-onset mutations may die *in utero* or during early postnatal life) and misdiagnosis frequently happens (for example confusion with Pompe disease, a glycogen storage disease), it is likely the incidence of *PRKAG2*-induced HCM is underreported. Our study revealed a mutation located in the CBS3 repeat, which has no previous reported mutation, and behaved quite differently in terms of changes in AMPK activity and allosteric activation from other *PRKAG2* mutations. Moreover, our data suggest that targeted therapy of *PRKAG2*-induced HCM using mTOR inhibition should be considered.

Our molecular studies in HEK293 cells show that the K475E mutation has three effects on the regulation of the AMPK complex: (i) markedly increasing the basal phosphorylation of T172 and hence basal kinase activity; (ii) reducing the sensitivity to AMP in allosteric activation; (iii) preventing the increase in T172 phosphorylation observed in response to phenformin, which increases cellular ADP:ATP and AMP:ATP ratios. The three nucleotide-binding sites (1, 3 and 4) in the AMPK- γ subunit are numbered by convention according to the number of the CBS repeat that carries an aspartate side chain interacting with the 2'- and 3'-hydroxyls of the nucleotide ribose ring (17). The structural analysis illustrated in Figure 4 suggests that K242 in γ 1 (equivalent to K475 in γ 2) is involved in forming electrostatic interactions with phosphate groups of all three adenine nucleotides, AMP, ADP and ATP, in site 1. Interestingly, a lysine at this position is conserved in all vertebrate γ 1 and γ 2 isoforms, and also in some invertebrate orthologues such as that from *Drosophila melanogaster*; in vertebrate γ 3 isoforms and many other invertebrate orthologues it is replaced by another basic residue, arginine. A basic residue at this position is not, however, conserved in the fungal and plant *Arabidopsis thaliana*, where allosteric activation by AMP is not observed (Figure 4D). The K475E mutation replaces the positively charged amine of lysine with the negatively charged carboxyl group of glutamate, potentially disrupting electrostatic interactions with all three nucleotides. Although it is difficult to predict the relative effects this might have on binding of the three nucleotides, if it had a larger effect on the binding of AMP than ATP it would be expected that higher concentrations of AMP would be required to displace ATP from site 1.

Consistent with this, the EC₅₀ for allosteric activation of the K475E mutant by AMP was around 15-fold higher than that of the wild type (Figure 2). The maximal degree of activation by AMP also appeared to be reduced, although analysis of this was hindered by the fact AMP starts to inhibit AMPK at concentrations above 200 μ M, due to competition with ATP at the catalytic site.

Xiao et al (32) originally proposed that the effects of AMP on allosteric activation were entirely due to binding at site 1, whereas the effects of AMP and/or ADP on T172 dephosphorylation were due to binding at site 3. Since K242 in γ 1 only seems to interact with nucleotides in site 1, the model of Xiao et al (32) is consistent with our data showing that the K475E mutation markedly affects allosteric activation by AMP (Figure 2B). However, there were also major effects of the K475E mutation to increase the basal T172 phosphorylation and hence basal activity, while preventing further phosphorylation induced by phenformin-triggered metabolic stress in intact cells. These effects observed in HEK293 cells are less easy to explain using the simple model of Xiao et al (32). The three nucleotide-binding sites in the γ subunit lie very close together, and the side chains of some conserved basic residues (e.g. H150 and H297 in rat γ 1) make interactions with the phosphate groups of more than one nucleotide (31). It is therefore not surprising that mutations affecting binding of a nucleotide at one site can also affect binding and function at other sites. For example, mutation to alanine of any one of the three aspartate residues that define sites 1, 3 and 4 (D89 in CBS1, D244 in CBS3 and D316 in CBS4, rat γ 1) affects not only allosteric activation but also T172 phosphorylation (24). That the model of Xiao et al (32) is an oversimplification is also suggested by a recent study in which a core AMPK complex was crystallized in the presence of ATP rather than AMP. In this structure, ATP was found in sites 1 and 4, with site 3 being empty; it was also suggested that the mode of ATP binding in site 4 would preclude binding of any nucleotide at site 3 (9). Xiao et al had previously proposed that site 4 was a “non-exchangeable” site at which AMP bound tightly and irreversibly (31). It is clear that the roles of the three γ subunit nucleotide-binding sites on AMPK function are complex, and remain incompletely understood.

Of the three effects of the K475E mutation on AMPK function, which is the most likely to cause the clinical problems for the patient? The K475E mutation causes both loss-of-function and gain-of-function effects. The loss-of-function effects are the reduced allosteric activation by AMP, and the reduced ability of cellular stresses such as phenformin to increase T172 phosphorylation as seen in both HEK293 and H9c2 cells. We suspect that these effects could be compensated for by

the $\gamma 1$ isoform, which is expressed along with $\gamma 2$ in developing and adult mouse heart, and adult human heart (19,26), and appears to account for about 80% of total AMPK activity in adult rat heart (13). Both the *de novo* and inherited mutations in the *PRKAG2* gene are dominant in effect, and increased basal activity and T172 phosphorylation have been previously reported for the R531G, R531Q and R384T mutations, with both of the latter being *de novo* mutations that caused severe disease leading to death in early life (1,8). Our study in H9c2 cells showed a significant reduction in T172 phosphorylation and reduced response to phenformin. Thus, cell environment appears to be important in studying this gene mutation. The K475E mutation induced inhibition of AMPK observed in H9c2 cells is in agreement with the structural modeling results where the mutation causes disruption of electrostatic interactions with adenine nucleotides. Activation of AMPK is well known to inhibit downstream signaling pathway, including the mTOR which plays a critical roles in regulation of cell growth. Since we observed a markedly increases in phosphorylation of p70S6K, S6 and 4E-BP1 in K475E expressing H9c2 cells and the patient with the mutation, a loss-of-function K475E phenotype seems logical.

mTOR functions by interacting with several adaptor proteins to form two distinct multiprotein complexes: mTOR complex 1 (mTORC1) and mTORC2. mTORC1 is a critical regulator of protein synthesis, cell growth and proliferation and many other metabolic processes (28). p70S6K is required for G1 cell cycle progression and cell growth. Phosphorylation of p70S6K is required for its activation and T389 is the principal regulatory phosphorylation site. 4E-BP1 is a translation repressor protein. It functions by binding to the eukaryotic translation initiation factor 4E (eIF4E). Only when being hyperphosphorylated would 4E-BP1 stop interaction with eIF4E which results in activation of cap-dependent translation (25). Since both p70S6K and 4E-BP1 are considered downstream of mTORC1 and can be phosphorylated by mTOR, we examined phosphorylation of these two critical signaling factors to determine changes in cell growth response by the K475E mutation. We observed significant increases in p70S6K phosphorylation at T389 as well as Ser-421/T424 sites with the K475E mutation. Not surprisingly ribosomal protein S6 phosphorylation (S235/S236 and S240/S244) was also significantly increased. A noted hyper-phosphorylation was also found with the K475E mutation. These changes were consistent in H9c2 cells as well as in the patient fibroblasts. These observations suggest that the K475E mutation induces activation of cell growth pathway downstream of mTOR. Our next step, logically, is to test the therapeutic potential

of mTOR inhibition in ameliorating *PRKAG2* mutation-induced changes *in vivo*. Using H9c2 cells we demonstrated that cell hypertrophy induced by the K475E mutation can be reversed by rapamycin. This is encouraging as to date there is no targeted therapy for *PRKAG2* HCM. Hence, the next step would be to develop transgenic mouse models to demonstrate the effectiveness of the mTOR inhibition strategy in treating *PRKAG2* mutation-induced HCM.

Overall, our data show that a novel, *de novo* K475E *PRKAG2* mutation causing hypertrophic cardiomyopathy. The K475E mutation induces changes in the AMPK complex that are not shared by the other *PRKAG2* mutations. The K475E mutation also induces activation of cell growth pathways and hypertrophy which can be effectively reversed by rapamycin treatment.

Acknowledgements:

This study was supported by NIH P30GM114750 [A.U., J.P. (Director), S.S, Y.-T.T.] and the Oh-Zopfi Research Award, Women & Infant's Hospital (C.P., Y.-T.T.). We thank the COBRE in Perinatal Biology Core and Kilguss Core Facility for the excellent flow cytometry and microscopy supports. The authors would also like to thank Dr. Umadevi Tantravahi, Director of Medical Genetics, Women & Infants Hospital, for providing the age- and sex-matched fibroblasts.

References

1. **Akman HO, Sampayo JN, Ross FA, Scott JW, Wilson G, Benson L, Bruno C, Shanske S, Hardie DG, Dimauro S.** Fatal infantile cardiac glycogenosis with phosphorylase kinase deficiency and a mutation in the gamma2-subunit of AMP-activated protein kinase. *Pediatr Res* 62(4):499-504, 2007.
2. **Arad M, Benson DW, Perez-Atayde AR, McKenna WJ, Sparks EA, Kanter RJ, McGarry K, Seidman JG, Seidman CE.** Constitutively active AMP kinase mutations cause glycogen storage disease mimicking hypertrophic cardiomyopathy. *J Clin Invest* 109(3):357-362, 2002.
3. **Arad M, Maron BJ, Gorham JM, Johnson WH Jr, Saul JP, Perez-Atayde AR, Spirito P, Wright GB, Kanter RJ, Seidman CE, Seidman JG.** Glycogen storage diseases presenting as hypertrophic cardiomyopathy. *N Engl J Med* 352(4):362-372, 2005.
4. **Bateman A.** The structure of a domain common to archaebacteria and the homocystinuria disease protein. *Trends Biochem Sci* 22(1):12-13, 1997.
5. **Bayrak F, Komurcu-Bayrak E, Mutlu B, Kahveci G, Basaran Y, Erginel-Unaltuna N.** Ventricular pre-excitation and cardiac hypertrophy mimicking hypertrophic cardiomyopathy in a Turkish family with a novel PRKAG2 mutation. *Eur J Heart Fail* 8(7):712-715, 2006.
6. **Blair E, Redwood C, Ashrafian H, Oliveira M, Broxholme J, Kerr B, Salmon A, Ostman-Smith I, Watkins H.** Mutations in the $\gamma 2$ subunit of AMP-activated protein kinase cause familial hypertrophic cardiomyopathy: evidence for the central role of energy compromise in disease pathogenesis. *Hum Mol Genet* 10(11):1215-1220, 2001.
7. **Burnett PE, Barrow RK, Cohen NA, Snyder SH, Sabatini DM.** RAFT1 phosphorylation of the translational regulators p70 S6 kinase and 4E-BP1. *Proc Natl Acad Sci U S A* 95(4):1432-7143, 1998.
8. **Burwinkel B, Scott JW, Bühner C, van Landeghem FK, Cox GF, Wilson CJ, Grahame Hardie D, Kilimann MW.** Fatal congenital heart glycogenosis caused by a recurrent activating

429 R531Q mutation in the gamma 2-subunit of AMP-activated protein kinase (*PRKAG2*), not by
 430 phosphorylase kinase deficiency. *Am J Hum Genet* 76(6):1034-1049, 2005.

431 9. **Chen L, Wang J, Zhang YY, Yan SF, Neumann D, Schlattner U, Wang ZX, Wu JW.** AMP-
 432 activated protein kinase undergoes nucleotide-dependent conformational changes. *Nat*
 433 *Struct Mol Biol* 19:716-718, 2012.

434 10. **Gollob MH, Green MS, Tang AS, Gollob T, Karibe A, Ali Hassan AS, Ahmad F, Lozado**
 435 **R, Shah G, Fananapazir L, Bachinski LL, Roberts R.** Identification of a gene responsible for
 436 familial Wolff-Parkinson-White syndrome. *N Engl J Med* 344(24):1823-1831, 2001.

437 11. **Gollob MH, Seger JJ, Gollob TN, Tapscott T, Gonzales O, Bachinski L, Roberts R.** Novel
 438 *PRKAG2* mutation responsible for the genetic syndrome of ventricular preexcitation and
 439 conduction system disease with childhood onset and absence of cardiac hypertrophy.
 440 *Circulation* 104(25):3030-3033, 2001.

441 12. **Hardie DG, Hawley SA.** AMP-activated protein kinase: the energy charge hypothesis revisited.
 442 *Bioessays* 23(12):1112-1119, 2001.

443 13. **Hawley SA, Davison M, Woods A, Davies SP, Beri RK, Carling D, Hardie DG.**
 444 Characterization of the AMP-activated protein kinase kinase from rat liver and identification of
 445 threonine 172 as the major site at which it phosphorylates AMP-activated protein kinase. *J Biol*
 446 *Chem* 271(44):27879-27887, 1996.

447 14. **Hawley SA, Ross FA, Chevtzoff C, Green KA, Evans A, Fogarty S, Towler MC, Brown**
 448 **LJ, Ogunbayo OA, Evans AM, Hardie DG.** Use of cells expressing gamma subunit variants
 449 to identify diverse mechanisms of AMPK activation. *Cell Metab* 11(6):554-565.

450 15. **Kahn BB, Alquier T, Carling D, Hardie DG.** AMP-activated protein kinase: ancient energy
 451 gauge provides clues to modern understanding of metabolism. *Cell Metab* 1(1):15-25, 2005.

452 16. **Kelly BP, Russell MW, Hennessy JR, Ensing GJ.** Severe hypertrophic cardiomyopathy in an
 453 infant with a novel *PRKAG2* gene mutation: potential differences between infantile and adult
 454 onset presentation. *Pediatr Cardiol* 30(8):1176-1179, 2009.

- 455 17. **Kemp BE, Oakhill JS, Scott JW.** AMPK structure and regulation from three angles. *Structure*
456 15:1161-1163, 2007.
- 457 18. **Kim M, Hunter RW, Garcia-Menendez L, Gong G, Yang YY, Kolwicz SC Jr, Xu J,**
458 **Sakamoto K, Wang W, Tian R.** Mutation in the γ 2-subunit of AMP-activated protein kinase
459 stimulates cardiomyocyte proliferation and hypertrophy independent of glycogen storage. *Circ*
460 *Res* 114(6):966-975, 2014.
- 461 19. **Kim M, Shen M, Ngoy S, Karamanlidis G, Liao R, Tian R.** AMPK isoform expression in the
462 normal and failing hearts. *J Mol Cell Cardiol* 52:1066-1073, 2012.
- 463 20. **Laforêt P, Richard P, Said MA, Romero NB, Lacene E, Leroy JP, Baussan C, Hogrel JY,**
464 **Lavergne T, Wahbi K, Hainque B, Duboc D.** A new mutation in *PRKAG2* gene causing
465 hypertrophic cardiomyopathy with conduction system disease and muscular glycogenosis.
466 *Neuromuscul Disord* 16(3):178-182, 2006.
- 467 21. **Liu Y, Bai R, Wang L, Zhang C, Zhao R, Wan D, Chen X, Caceres G, Barr D, Barajas-**
468 **Martinez H, Antzelevitch C, Hu D.** Identification of a novel de novo mutation associated with
469 *PRKAG2* cardiac syndrome and early onset of heart failure. *PLoS One* 8(5):e64603, 2013.
- 470 22. **Luptak I, Shen M, He H, Hirshman MF, Musi N, Goodyear LJ, Yan J, Wakimoto H,**
471 **Morita H, Arad M, Seidman CE, Seidman JG, Ingwall JS, Balschi JA, Tian R.** Aberrant
472 activation of AMP-activated protein kinase remodels metabolic network in favor of cardiac
473 glycogen storage. *J Clin Invest* 117:1432-1439, 2007.
- 474 23. **Morita H, Rehm HL, Menesses A, McDonough B, Roberts AE, Kucherlapati R, Towbin**
475 **JA, Seidman JG, Seidman CE.** Shared genetic causes of cardiac hypertrophy in children and
476 adults. *N Engl J Med* 358(18):1899-1908.
- 477 24. **Oakhill JS, Chen ZP, Scott JW, Steel R, Castelli LA, Ling N, Macaulay SL, Kemp BE.** β -
478 Subunit myristoylation is the gatekeeper for initiating metabolic stress sensing by AMP-
479 activated protein kinase (AMPK). *Proc Natl Acad Sci USA* 107:19237-19241, 2010.

- 480 25. **Pause A, Belsham GJ, Gingras AC, Donzé O, Lin TA, Lawrence JC Jr, Sonenberg N.**
481 Insulin-dependent stimulation of protein synthesis by phosphorylation of a regulator of 5'-cap
482 function. *Nature* 371(6500):762-767, 1994.
- 483 26. **Pinter K, Grignani RT, Czibik G, Farza H, Watkins H, Redwood C.** Embryonic expression
484 of AMPK gamma subunits and the identification of a novel $\gamma 2$ transcript variant in adult heart. *J*
485 *Mol Cell Cardiol* 53:342-349, 2012.
- 486 27. **Pöyhönen P, Hiippala A, Ollila L, Kaasalainen T, Hänninen H, Heliö T, Tallila J,**
487 **Vasilescu C, Kivistö S, Ojala T, Holmström M.** Cardiovascular magnetic resonance findings
488 in patients with *PRKAG2* gene mutations. *J Cardiovasc Magn Reson* 17:89, 2015.
- 489 28. **Sciarretta S, Volpe M, Sadoshima J.** Mammalian target of rapamycin signaling in cardiac
490 physiology and disease. *Circ Res* 114(3):549-564, 2014.
- 491 29. **Scott JW, Hawley SA, Green KA, Anis M, Stewart G, Scullion GA, Norman DG, Hardie**
492 **DG.** CBS domains form energy-sensing modules whose binding of adenosine ligands is
493 disrupted by disease mutations. *J Clin Invest* 113:274– 284, 2004.
- 494 30. **Watkins SJ, Borthwick GM, Arthur HM.** The H9C2 cell line and primary neonatal
495 cardiomyocyte cells show similar hypertrophic responses in vitro. *In Vitro Cell Dev Biol Anim*
496 47(2):125-131, 2011.
- 497 31. **Xiao B, Heath R, Saiu P, Leiper FC, Leone P, Jing C, Walker PA, Haire L, Eccleston JF,**
498 **Davis CT, Martin SR, Carling D, Gamblin SJ.** Structural basis for AMP binding to
499 mammalian AMP-activated protein kinase. *Nature* 449:496-500, 2007.
- 500 32. **Xiao B, Sanders MJ, Underwood E, Heath R, Mayer FV, Carmena D, Jing C, Walker PA,**
501 **Eccleston JF, Haire LF, Saiu P, Howell SA, Aasland R, Martin SR, Carling D, Gamblin**
502 **SJ.** Structure of mammalian AMPK and its regulation by ADP. *Nature* 472:230-233, 2011.
- 503 33. **Yano N, Ianus V, Zhao TC, Tseng A, Padbury JF, Tseng YT.** A novel signaling pathway for
504 β -adrenergic receptor-mediated activation of phosphoinositide 3-kinase in H9c2
505 cardiomyocytes. *Am J Physiol Heart Circ Physiol* 293(1):H385-H393.

34. **Zhang BL, Xu RL, Zhang J, Zhao XX, Wu H, Ma LP, Hu JQ, Zhang JL, Ye Z, Zheng X, Qin YW.** Identification and functional analysis of a novel PRKAG2 mutation responsible for Chinese PRKAG2 cardiac syndrome reveal an important role of non-CBS domains in regulating the AMPK pathway *J Cardiol* 62(4):241-248, 2013.
35. **Zhang BL, Ye Z, Xu RL, You XH, Qin YW, Wu H, Cao J, Zhang JL, Zheng X, Zhao XX.** Overexpression of G100S mutation in PRKAG2 causes Wolff-Parkinson-White syndrome in zebrafish. *Clin Genet* 86(3):287-291, 2014.

Figure Legends:

Figure 1. Amino acid alignment of γ 2-subunit of AMPK and echocardiogram of the patient with the K475E mutation. (A) Family pedigree of the *PRKAG2* K475E carrier. (B) Lysine at 475 position in the CBS3 repeat of the γ 2 isoform of AMPK is conserved among all species. A K485E mutation at the linker region between CBS3 and CBS4 was recently reported (21). (C) The echocardiogram was taken at 7 month old when the patient was being treated for hypertrophy cardiomyopathy.

Figure 2. Effects of the K475E mutation on activity of AMPK in HEK-293 cells. (A) Effect of AMP on absolute AMPK activity. HEK-293 cells stably expressing FLAG-tagged wild type (WT) γ 2 or a K475E mutant were lysed, AMPK immunoprecipitated using anti-FLAG antibodies and kinase activity assayed at different AMP concentrations. Data (mean \pm SEM, triplicate assays) were fitted to the equation: $Y = \text{basal} + (((\text{activation} * \text{basal} - \text{basal}) * X) / (EC_{50} + X)) - (((\text{activation} * \text{basal}) * X) / (IC_{50} + X))$, where Y is activity, X is AMP concentration, EC_{50} is the concentration of AMP giving half-maximal activation and IC_{50} is the concentration of AMP giving half-maximal inhibition (AMP inhibits at high concentration due to competition with ATP at the catalytic site). The curves were generated by the following best-fit parameters: WT: basal = 0.027 ± 0.002 nmol/min/mg, activation = 3.9 ± 0.4 -fold, $EC_{50} = 6.2 \pm 2.0$ μ M, $IC_{50} = 1.5 \pm 0.5$ mM; K475E: basal = 0.21 ± 0.01 nmol/min/mg, activation \approx 2-fold, $EC_{50} \approx 100$ μ M, $IC_{50} \approx 1$ mM. (B) Effect of AMP on relative AMPK activity. As (A), but expressing kinase activity relative to the activity in the absence of AMP.

Figure 3. Effects of the K475E mutation on response to phenformin treatment in HEK-293 cells. Cells stably expressing FLAG-tagged wild type (WT) γ 2, R531G or K475E mutants were treated with or without phenformin (1.25 mM) for 1 hr, AMPK immunoprecipitated using anti-

FLAG antibody and assayed at 200 μ M AMP (upper panel). The lower panel shows the signal obtained using anti-pT172 antibody by Western blotting of immunoprecipitates and expressed relative to the signal obtained using anti-FLAG antibody. Data are mean \pm SEM (n = 3) and statistical significance determined by 1-way ANOVA (*P < 0.05, **P < 0.01, ***P < 0.001). ns, not significant.

Figure 4. Structural analysis of the role of the equivalent K242 residue in rat γ 1, and sequence conservation around K475 in AMPK isoforms. Models of rat γ 1 showing the relationship of D89, H150, R223 and K242 with bound AMP (**A**), ADP (**B**) and ATP (**C**) using RCSB Protein Data Bank ID 2V8Q, 2Y8L and 2V9J, respectively (24, 30; www.rcsb.org). Models were constructed using MacPyMol molecular visualization system with CBS1 (cyan), CBS2 (magenta), CBS3 (blue) and CBS4 (orange) in “cartoon” representation and nucleotides and highlighted residues in stick representation (C atoms in grey in side chains and green in nucleotides; O atoms blue, N atoms red, P atoms orange). (**D**) Alignment of sequences around K475 in human γ 2 and equivalent residues in other species and isoforms.

Figure 5. Overexpression of the K475E mutant in H9c2 cells results in AMPK inhibition and hypertrophy. H9c2 cells were stably transfected with the human *PRKAG2* wild type (WT) or the K475E mutant construct. (**A**) Cells were treated with vehicle or phenformin (1.25 mM) for 1, 4 or 24 hours. Shown are representative Western blots with antibody against phospho- AMPK α (T172) or AMPK α . (**B**) Densitometric scanning results of Western blots were shown in (A). Each bar represents measurement of phospho- AMPK α normalized with AMPK α from 3-4 separate experiments. * P < 0.05 vs. vehicle control within each gene expression group. # P < 0.05 vs. vehicle control of WT group. (**C**) Cells were trypsinized and analyzed by flow cytometry. Forward

scatter (FSC) was used to determine relative cell volume. Ten thousand cells each were analyzed for WT- (white histogram) and the K475E mutant-expressing (shaded histogram) cells.

Figure 6. Overexpression of the K475E mutant in H9c2 cells induces activation of cell growth signaling pathways. H9c2 cells were stably transfected with the human *PRKAG2* wild type (WT) or the K475E mutant construct. Shown are representative Western blots performed on cell lysates with an antibody against phospho- p70S6K (T389), phospho- p70S6K (T421/S424), phospho- S6 (S235/S236), phospho- S6 (S240/S244), phospho- 4E-BP1 (T37/T46), phospho- 4E-BP1 (S65), phospho- 4E-BP1 (T70), phospho- AKT (S473), or phospho- AKT (T308). Blots of each individual total protein (p70S6K, S6, 4E-BP1, AKT) were also included. **Densitometric scanning results of Western blots of H9c2 cells overexpressing human wild type (WT) or the K475E mutant *PRKAG2*.** Each bar represents measurement of each phospho-specific antibody normalized with its individual total antibody from 3-4 separate experiments. * $P < 0.05$ vs. individual WT.

Figure 7. Primary fibroblasts from the patient with the K475E mutation show activated cell growth signaling pathways. Fibroblasts from the patient with the K475E mutation and multiple controls were cultured. Western blots were performed on cell lysates with an antibody against phospho- p70S6K (T389), phospho- p70S6K (T421/S424), phospho- S6 (S235/S236), phospho- S6 (S240/S244), phospho- 4E-BP1 (T37/T46), phospho- 4E-BP1 (S65), phospho- 4E-BP1 (T70), phospho- AKT (S473), or phospho- AKT (T308). Blots of each individual total protein (p70S6K, S6, 4E-BP1, AKT) were also included. **Densitometric scanning results of Western blots of primary fibroblasts from the patient with the K475E mutation and multiple age- or/and sex-matched controls.** Each bar represents measurement of each phospho-specific antibody normalized with its individual total antibody from 3-4 separate experiments. * $P < 0.05$ vs. individual WT.

Figure 8. Angiotensin II (Ang II) induces H9c2 cell hypertrophy which can be reversed by rapamycin treatment. (A) H9c2 cells overexpressing the human *PRKAG2* wild type (WT) or the K475E mutant were treated with vehicle (Control), 200 nM Ang II, 50 nM rapamycin or Ang II in combination with rapamycin for 24 hours before stained for green fluorescent Calcein AM for microscopic assessment of cell area. **(B)** The bar graphs show the quantification results (n = 60-80 cells) from four individual experiments. * P < 0.05 vs. WT within the same treatment group. + P < 0.05 vs. vehicle control.

Figure 9. Hypertrophy phenotype induced by overexpression of the K475E mutant in H9c2 cells can be corrected by rapamycin treatment. (A) H9c2 cells overexpressing the human *PRKAG2* wild type (WT) or the K475E mutant were treated with vehicle (Control) or 50 nM rapamycin for the indicated period of time. Cell area was assessed as described in Figure 8. Each bar represents measurement of cell area from three to four separate experiments (n = 60-80 cells). * P < 0.05 vs. individual control of the same genotype and treatment day group. **(B)** The time- course effect of rapamycin treatment presented as cell area reduction (%) based on the data in **(A)**.

610

Table 1. Known human *PRKAG2* mutations and their cardiac phenotypes

	N-	CBS1	L1		CBS2			L2
	G100S	R302Q	M335T	H344P	H383R	R384T	T400N	
Early onset					X	X		
AMPK activity	↓					↑		
Myofibrillar disarray								
Reference	34, 35	2, 10		27	6	1	2	

611

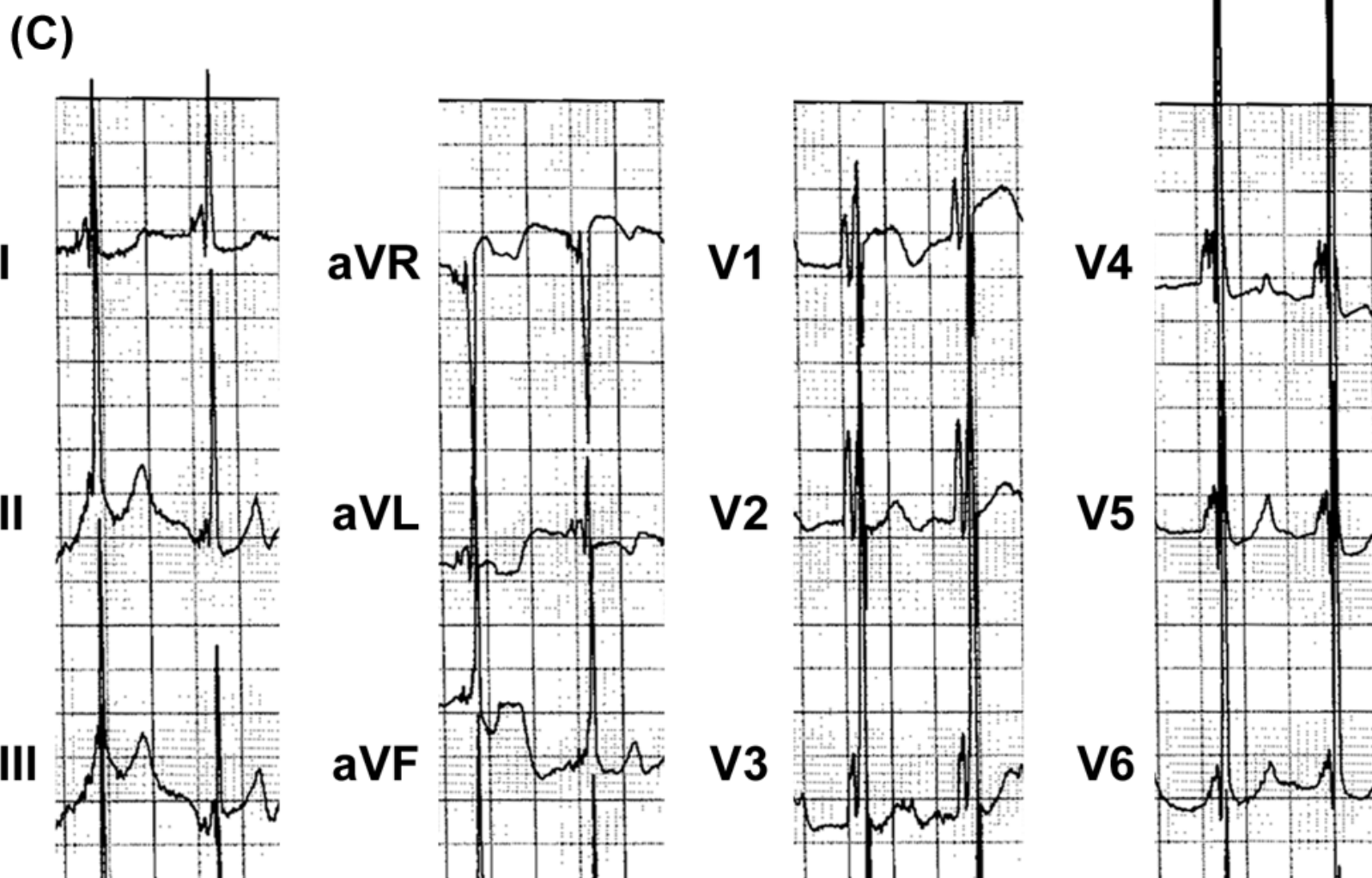
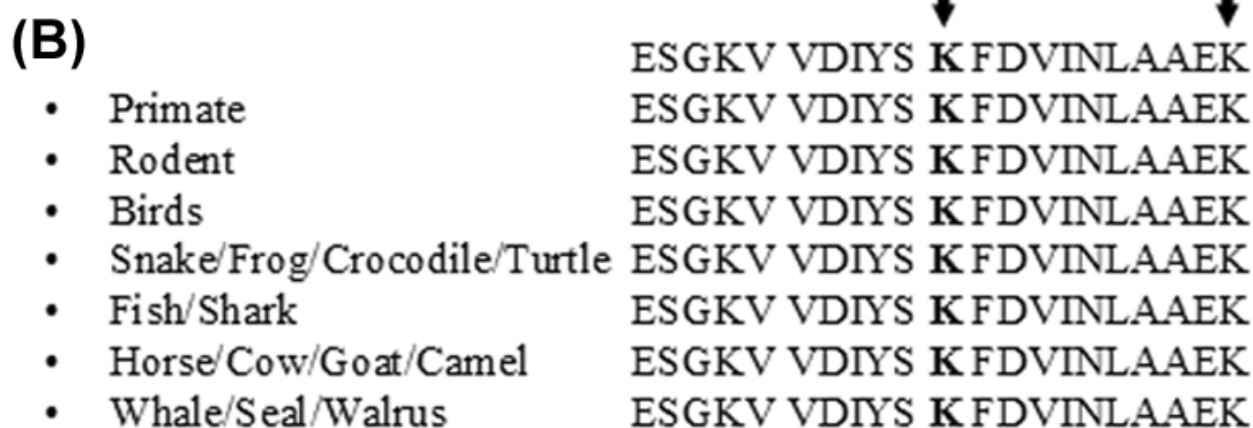
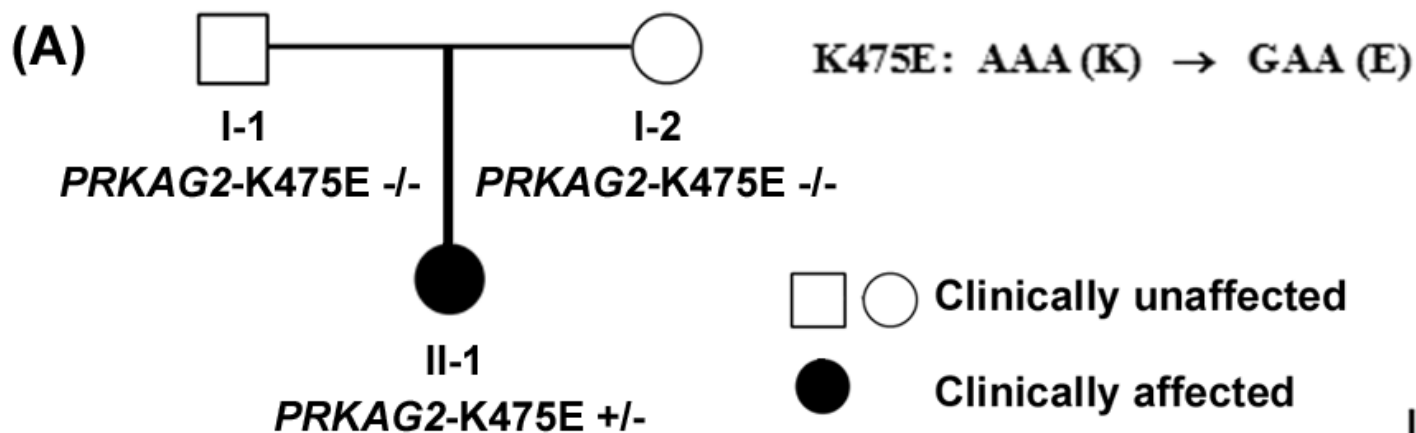
	CBS3	L3			CBS4						C-
	K475E	K485E	Y487H	N488I	E506K	E506K *	H530R	R531G #	R531Q	S548P	
Early onset	X					X	X	X	X		
AMPK activity	↓							↑	↑		
Myofibrillar disarray	?	X							X		
Reference		21	3	2, 22	5	16	23	11	8	20	

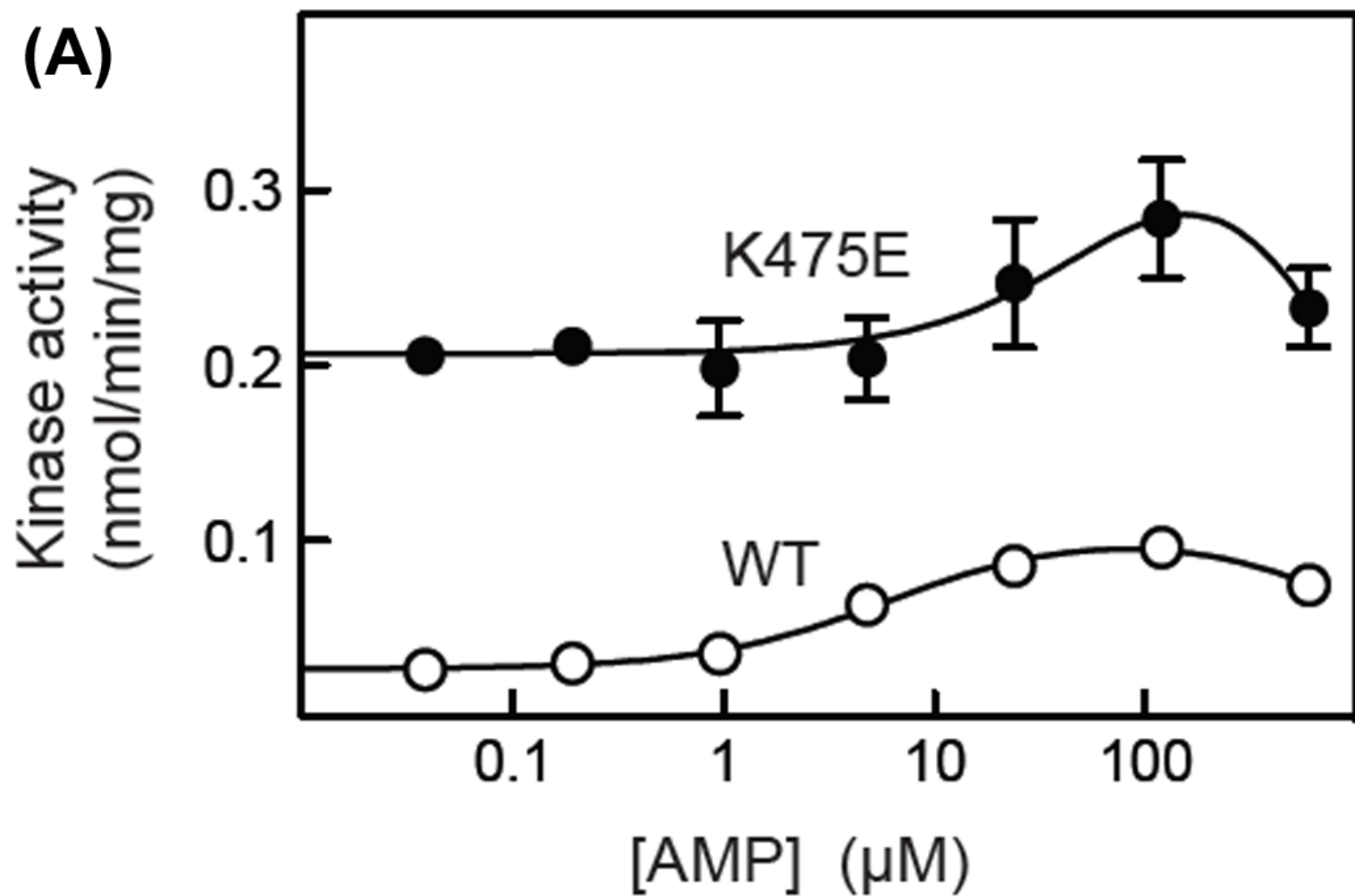
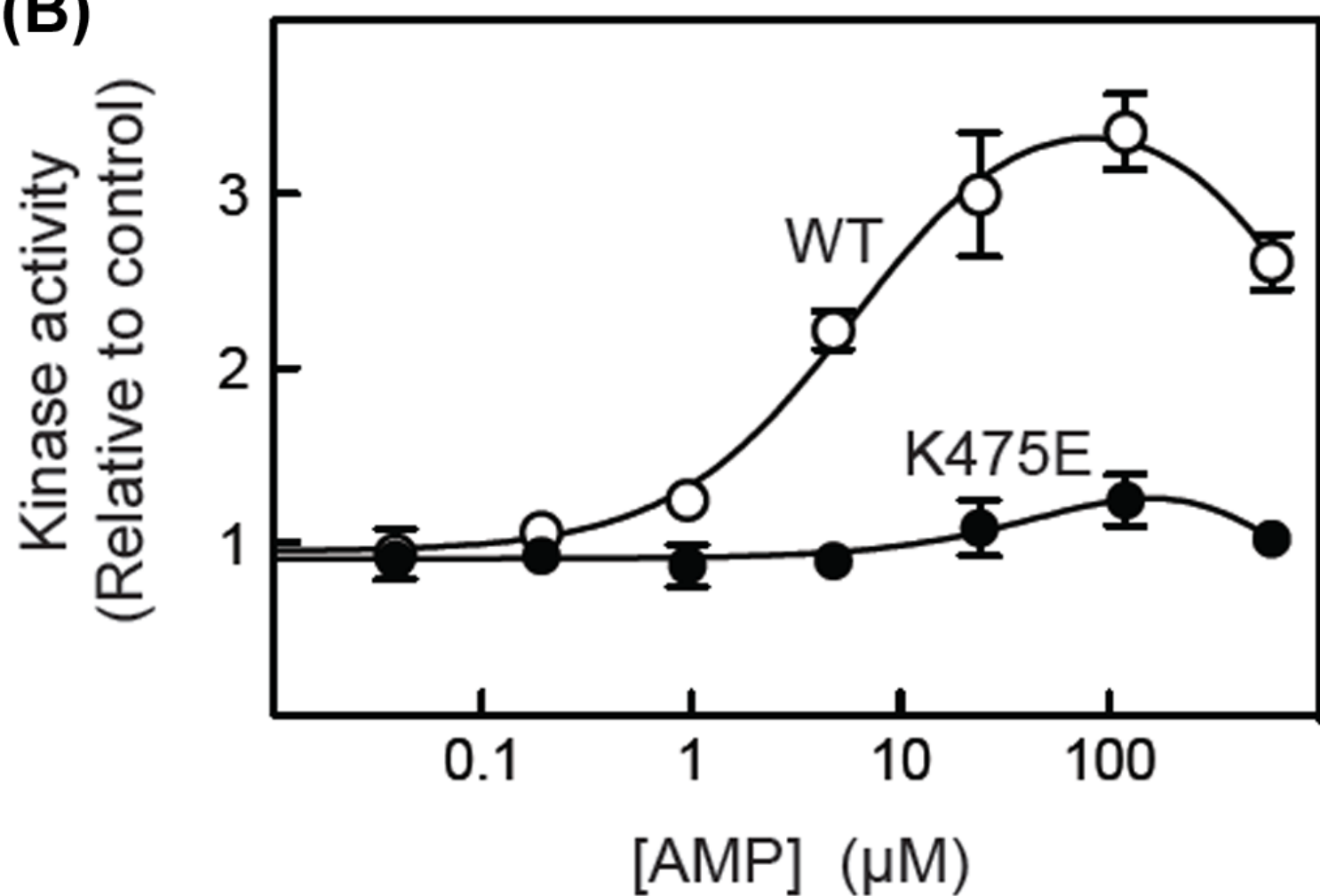
612 L, linker region.

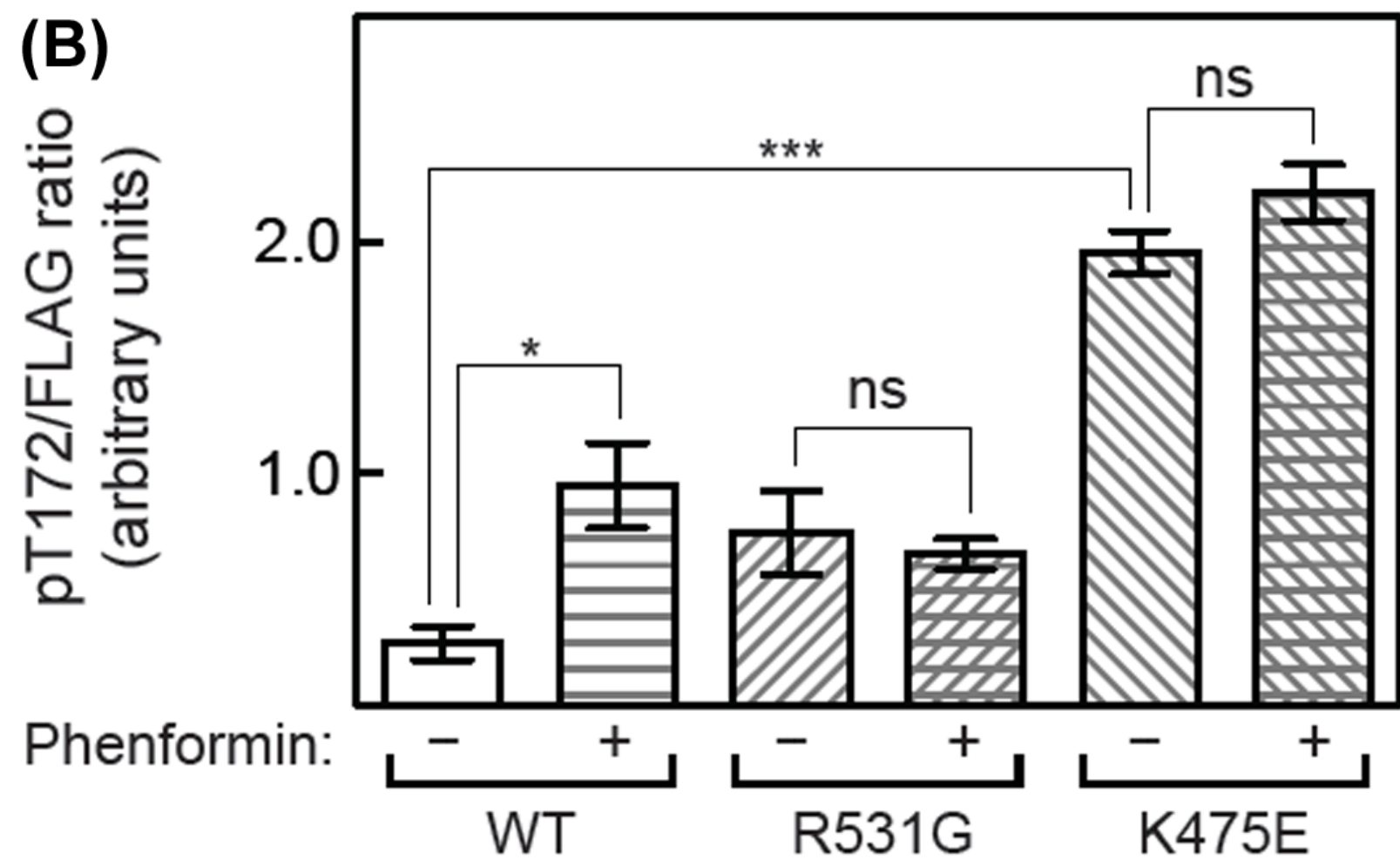
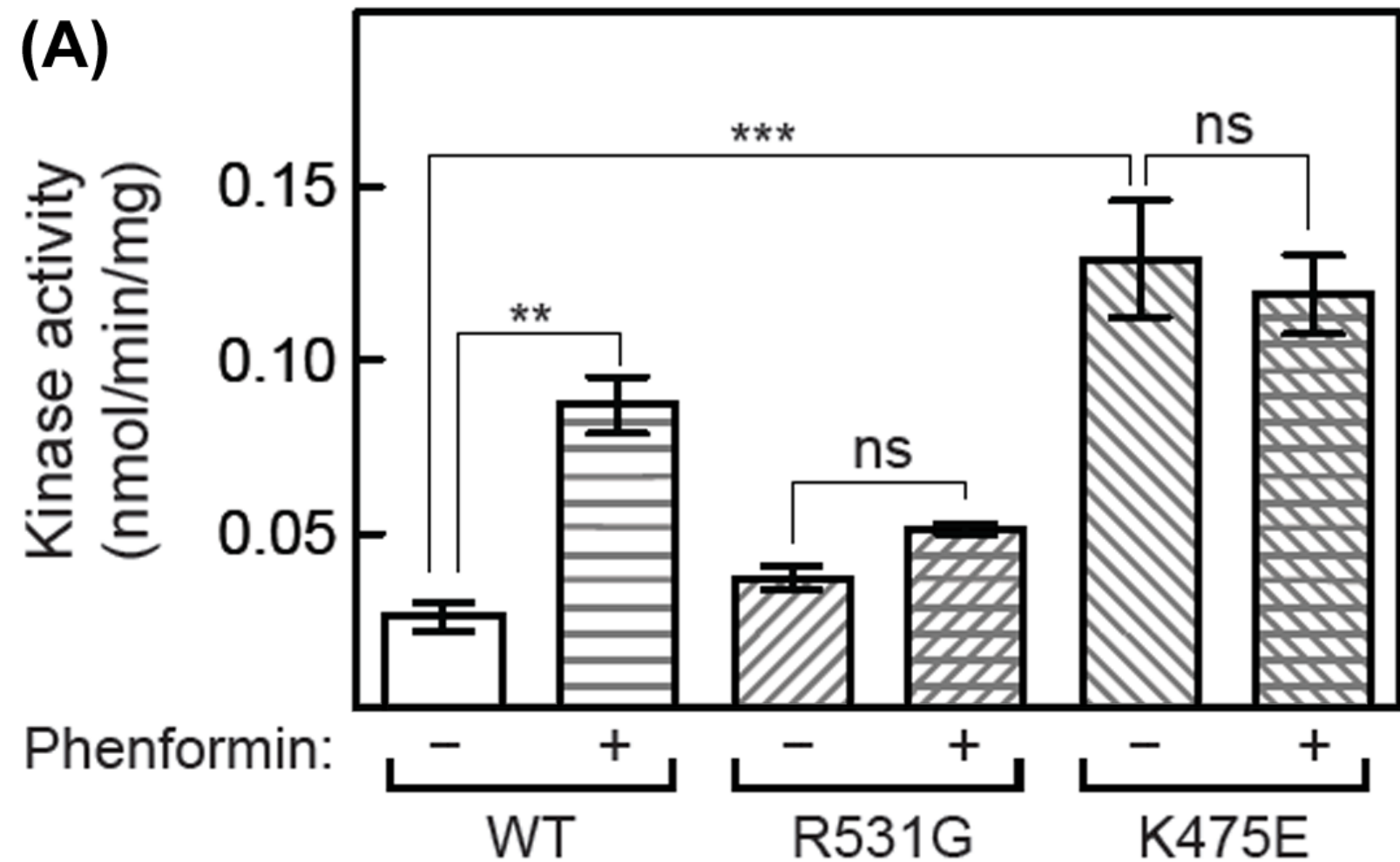
613 * No significant glycogen accumulation

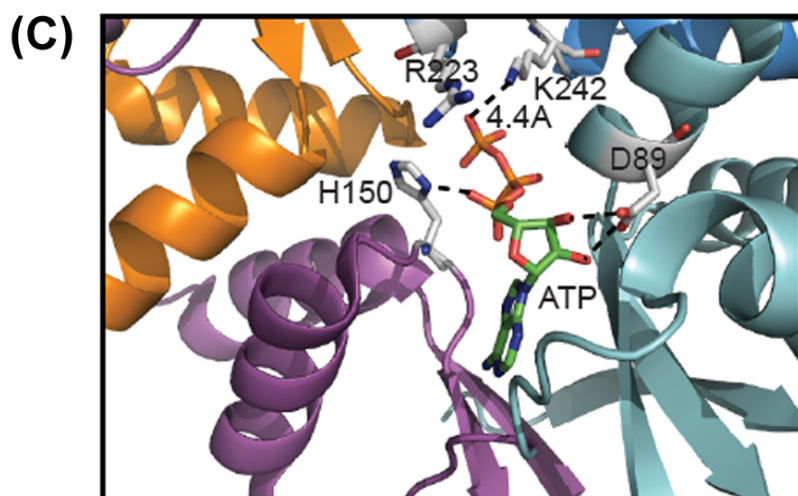
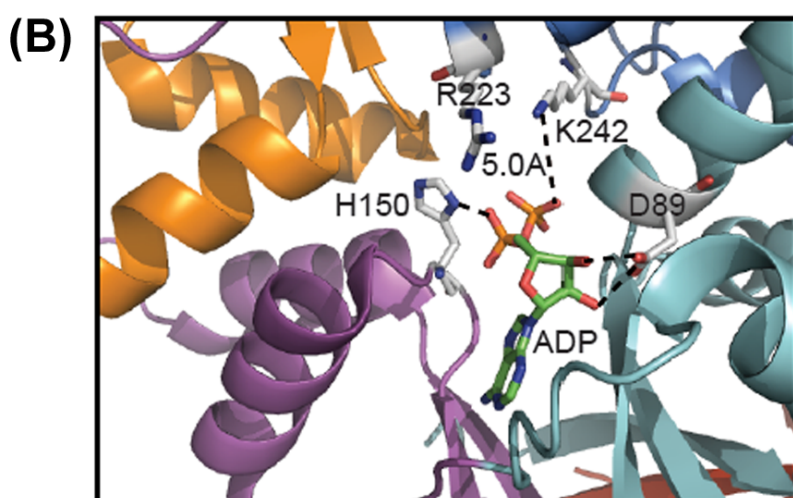
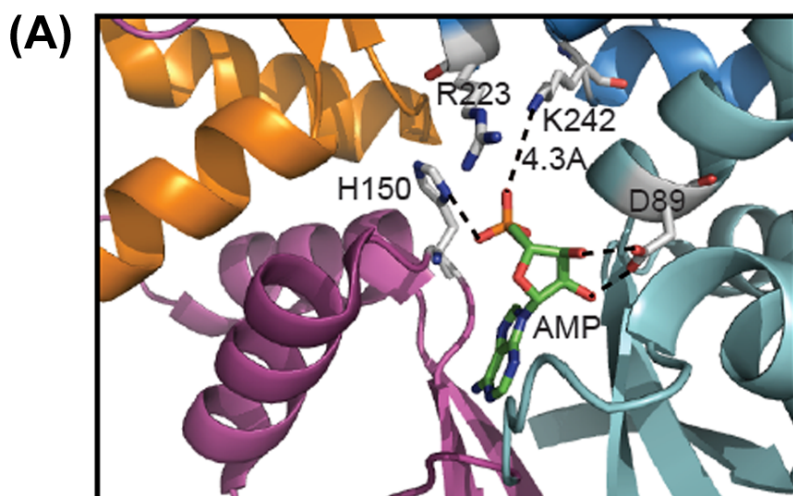
614 # No hypertrophy

615



(A)**(B)**





(D) *Homo sapiens* γ 1: RVVDIYS**K**FDVINLAA
Gallus gallus γ 1: RVVDIYS**K**FDVINLAA
Homo sapiens γ 2: KVVDIYS**K**FDVINLAA
Gallus gallus γ 2: KVVDIYS**K**FDVINLAA
Homo sapiens γ 3: QVVGLYS**R**FDVIHLAA
Gallus gallus γ 3: QVVGLYS**R**FDVIHLAA
D. melanogaster γ : RLVDIYA**K**FDVINLAA
C. elegans γ 1: RVVDIYA**K**FDVISLAA
Giardia lamblia γ : PPEEVL**R**KIEVLESAN
S. pombe γ : TLLNVYESVDVMHLIQ
S. cerevisiae Snf4: YLINVYEAYDVLGLIK
Arabidopsis thaliana γ : SLRDVQFLLTAPEIYH

